

## A Phasor Measurement Unit Based Fast Real-time Oscillation Detection Application for Monitoring Wind-farm-to-grid Sub-synchronous Dynamics

Luigi Vanfretti, Maxime Baudette, José-Luiz Domínguez-García, Muhammad Shoaib Almas, Austin White & Jan Ove Gjerde

To cite this article: Luigi Vanfretti, Maxime Baudette, José-Luiz Domínguez-García, Muhammad Shoaib Almas, Austin White & Jan Ove Gjerde (2016) A Phasor Measurement Unit Based Fast Real-time Oscillation Detection Application for Monitoring Wind-farm-to-grid Sub-synchronous Dynamics, *Electric Power Components and Systems*, 44:2, 123-134, DOI: [10.1080/15325008.2015.1101727](https://doi.org/10.1080/15325008.2015.1101727)

To link to this article: <https://doi.org/10.1080/15325008.2015.1101727>



Published online: 03 Dec 2015.



Submit your article to this journal [↗](#)



Article views: 338



View Crossmark data [↗](#)



Citing articles: 4 View citing articles [↗](#)

# A Phasor Measurement Unit Based Fast Real-time Oscillation Detection Application for Monitoring Wind-farm-to-grid Sub-synchronous Dynamics

Luigi Vanfretti,<sup>1,4</sup> Maxime Baudette,<sup>1</sup> José-Luiz Domínguez-García,<sup>2</sup>  
Muhammad Shoaib Almas,<sup>1</sup> Austin White,<sup>3</sup> and Jan Ove Gjerde<sup>4</sup>

<sup>1</sup>Smart Transmission System Laboratory (SmarTSs Lab), Electric Power Systems, KTH Royal Institute of Technology, Stockholm, Sweden

<sup>2</sup>Institute for Energy Research (IREC), Electrical Engineering Area, Spain

<sup>3</sup>Oklahoma Gas & Electric, Tennessee, USA

<sup>4</sup>Research and Development Division, Statnett SF, Norway

## CONTENTS

- 1. Introduction
- 2. Algorithms for Fast Oscillation Detection
- 3. Monitoring Application
- 4. Validation Experiments
- 5. Conclusion
- Funding
- References

---

**Abstract**—The increase of wind power share increasing has led to operational challenges for its integration and impact on power grids. Regarding this, unexpected dynamic phenomena, such as oscillatory events around 13 Hz, among different wind farms were recorded in the United States Oklahoma Gas & Electric. Such interactions differ from traditional inter-area oscillations, and the ability to detect them is the beyond measurement capabilities of most of existing measurement equipment and monitoring tools in energy management systems. This article presents the development and implementation of algorithms for fast sub-synchronous oscillation detection, focusing on the aforementioned case. It proposes a real-time monitoring application that exploits synchronized phasor measurements, allowing real-time detection of sub-synchronous wind farm dynamics. This tool was built as a prototype for real-time application and utilizes phasor measurement unit data for enhanced monitoring and control. The article focuses on the tool's design and its algorithms. Also, it will briefly present three approaches carried out for testing and validating the phasor measurement unit based application, one of which compares the proposed tool with an existing tool at Oklahoma Gas & Electric. Through such experiments, the tool presented in the article has been positively validated for real-time applications.

---

## 1. INTRODUCTION

Recent concerns about the environmental impact of traditional electricity generation in Western countries has led to a strong increase in renewable sources of energy. Since the 1990s, wind power has been the fastest growing power generation technology [1], a trend expected to continue as several countries have politically engaged themselves into large investments in wind power [2, 3].

Wind power is one kind among different intermittent generation sources that brings several challenges to power

Keywords: power system oscillations, monitoring application, PMU, wind farm, sub-synchronous oscillations

Received 22 December 2014; accepted 17 September 2015

Address correspondence to Dr. Luigi Vanfretti, Electric Power Systems, Teknikringen 33, SE-100 44, Stockholm, Sweden. E-mail: luigiv@kth.se

Color versions of one or more of the figures in the article can be found online at [www.tandfonline.com/uemp](http://www.tandfonline.com/uemp).

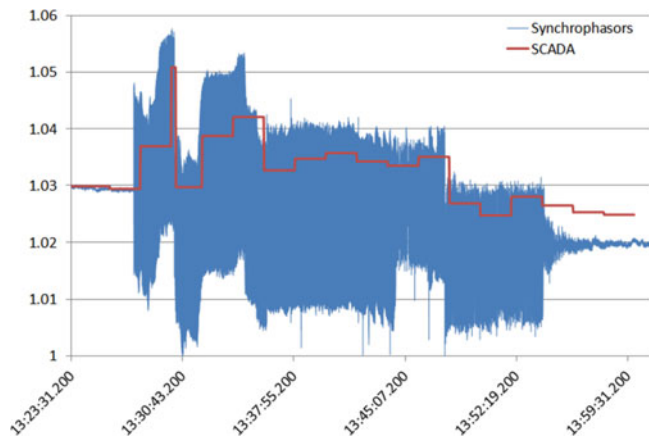


**FIGURE 1.** Comparison example between PMU measurements and SCADA data during a fast dynamic event; grid voltage is in p.u.

system dynamics. For example, its integration in existing power systems can involve transient stability issues [4]. Unexpected dynamic behavior is now appearing in the form of sub-synchronous oscillations. Oklahoma Gas & Electric (OG&E) has recently measured with phasor measurement units (PMUs) [5] sub-synchronous oscillatory events resulting from interactions between wind farms at frequencies around 3–15 Hz. These oscillations were also observed at the consumer level in the form of flicker [6].

Traditional monitoring tools built on supervisory control and data acquisition (SCADA) systems cannot detect these fast dynamics, due to low sampling frequencies and lack of time synchronization of primary measurement sources. Figure 1 presents a comparison between SCADA and PMU measurements for this phenomenon. The usage of PMUs enables observability for phenomena occurring at frequencies up to half the reporting rate of these instruments (*e.g.*, 15/25 Hz for a 30/50 samples per second reporting rate), opening new and wide perspectives for monitoring and control applications based on synchrophasors. These new tools will help in acquiring a better knowledge on the challenges brought by the increase of intermittent energy sources.

This article presents a PMU-based monitoring tool developed for detecting sub-synchronous oscillatory phenomena in power systems with a high wind power plant presence, similar to the one operated by OG&E. Moreover, the tool was tested and validated using three different types of experiments, including a comparison with an existing detection tool, and both hardware-in-the-loop (HIL) real-time simulation and real hardware-based emulation tests. The results obtained from these different types of tests demonstrate the good performance of the tool for allowing PMU-systems to detect sub-synchronous oscillations in power systems with a high wind plant presence, such as OG&E's.

## 2. ALGORITHMS FOR FAST OSCILLATION DETECTION

The effects of high frequency oscillations presented in the Section 1 are undesirable [5]; monitoring algorithms should therefore enable fast oscillation detection from PMU measurements. Traditional monitoring tools for inter-area oscillations estimate the frequency and damping for each oscillatory mode with two separate algorithms. However, this estimation process will require several seconds to obtain accurate frequency and damping estimates

Detection of sub-synchronous oscillations such as those described in Section 1 is a different problem, as the main requirement is to provide quick detection of the unexpected dynamics in a given frequency range. Hence, the proposed tool in this article uses one algorithm dedicated to the estimation of the amount of energy in the oscillations and the others dedicated to frequency estimation. The first is used to provide fast detection, and the second is used to provide usual confirmation of the detection results.

The three main algorithms used by the proposed PMU application (fast oscillation detection, frequency estimation, and pre-processing) are described next.

### 2.1. Fast Oscillation Detection

The proposed oscillation detection algorithm in this article builds from work in [7]. As highlighted in [8], it is desirable for a fast oscillation detection tool to provide information about oscillatory behavior at different bands of the spectrum, without necessarily pinpointing the specific dynamics active in the given band. Thus, the fast oscillation detection algorithm included in the tool allows providing a measure of the severity of the oscillatory behavior. The spectrum of frequency of interest with potential oscillatory activity goes from 0.1 Hz up to 50 or 60 Hz. However, such maximum frequency cannot be reached due to the PMU reporting rate and the Nyquist–Shannon criterion. To cover such a broad span of frequencies, the algorithm can be executed in parallel several times; four instances in this case are shown in Fig. 2. Each instance can be configured independently and thus monitor different frequency ranges. The following ranges, which depend on the sub-synchronous oscillation frequency, are suggested for the tool configuration:

- 0.10–1 Hz: Inter-area modes, *e.g.*, system-wide electromechanical swings;
- 1–3 Hz: local-area and torsional modes;
- 3–15 Hz: high-frequency oscillations, *e.g.*, wind farms controller interactions; and

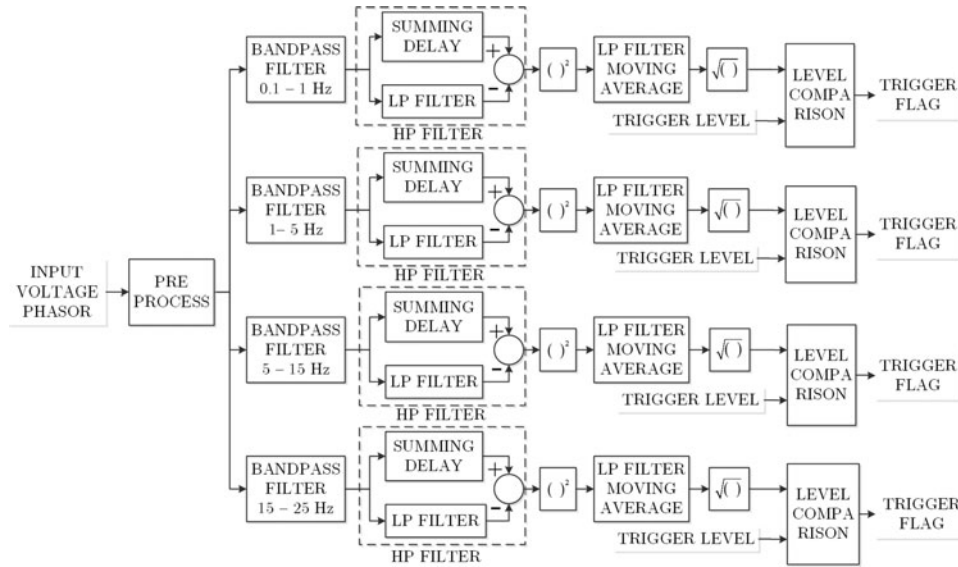


FIGURE 2. Diagram of the algorithm for fast real-time oscillation detection.

- 15–25 Hz: other sub-synchronous oscillations, e.g., sub-synchronous resonance.

As shown in Fig. 2, after pre-processing the real-time measurements, each frequency range previously mentioned is separated by four different band-pass filters set to the boundary frequencies of each range. This allows rapid determination of the type of oscillation detected.

The output of the high-pass filter provides a measure of the “oscillatory activity” at the selected frequency range. The root mean square (RMS) value of this output is used for energy computation, implying that the following computations are performed sequentially: squaring, averaging, and finally computing the square-root of the signal. A low-pass moving average filter is used to extract the main trend of the squared signal. This is necessary so that a persistent and stable signal is provided to the forthcoming trigger level comparison. Finally, a trigger level comparison indicates if the computed energy exceeds a pre-set level.

### 2.2. Frequency Estimation

The frequency estimation algorithm, depicted in Fig. 3, is composed of two different algorithms running in parallel. In this algorithm, the user may choose to activate one of them or both simultaneously. Depending on the case, the user may prefer to use a different method. A non-parametric method can be used when the frequency of the oscillations within a certain range is unknown, whereas a parametric method is appropriate when the knowledge about the number of possible oscillations within a range is known.

A brief description of both methods implemented is given in the following section.

#### 2.2.1. Non-parametric Welch’s Method

Welch’s power spectrum estimation is a method based on the standard periodogram. The method attempts to increase the readability of the power spectrum density (PSD) by reducing the noise; however, it decreases the frequency resolution.

The method works as follows.

1. The input signal is split into overlapping segments of length  $M$  (the overlapping rate is set by the user).
2. Each segment is windowed (the window is chosen by the user).
3. The fast Fourier transform (FFT) is computed for each windowed segment.
4. The PSD is obtained by averaging all the resulting spectra, thereby reducing the final variance.

For a complete description of the method, refer to Peter Welch’s original article [9].

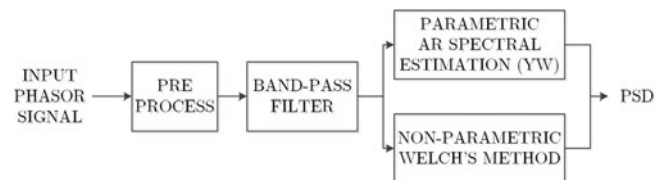


FIGURE 3. Diagram of the algorithm for spectral estimation.

Since this method is based on FFT computations, it will highlight all the content of the power frequency spectrum, which is an intrinsic property of non-parametric estimation. This property is especially useful for signals for which the actual frequency content is unknown.

### 2.2.2. Parametric Auto-regressive Methods

These methods use an auto-regressive mathematical model of the input signal for estimating power spectral density. In this way, they integrate available knowledge about the input signal to improve spectral estimation.

Auto-regressive models have been applied for estimating power system frequency content, as described in [10, 11]. For this specific reason, this model is chosen in the *monitoring tool*. The specific method utilized is left to the choice of the user. All of the implemented methods work on the principle of model fitting. They differ on the method used to optimize the fitting process. For further details on parametric methods, refer to [12], and for further details on their application to power systems, refer to [11]. It is worth mentioning that during experimentations, the Burg lattice method has been particularly efficient.

The order of the model is a very important parameter. Its value cannot be fixed in advance because it is mainly dependent on the number of oscillations to be identified and, thus, the frequency content itself. In the case of the Monitoring Tool where the frequency spectrum of interest is divided into four frequency ranges, the order can be different in each of the frequency bands. It is worth mentioning that too small orders will lead to a smooth spectrum and some modes might be left unidentified (under-fitting). On the other hand, too large orders might lead to the identification of artificial modes and their appearance on the estimated spectrum (over-fitting).

### 2.3. Data Pre-Processing: Outlier Removal and Down Sampling

The algorithms for estimating the energy and frequency of oscillations described previously involve filtering, averaging, and spectral estimation processes. These processes require reliable data. In the case of PMUs, measurements are reported at a rather high rate (30, 50, or 60 samples per second), transmitted over IP networks, and might contain wrong or missing measurements. The pre-processing of input data thus appears necessary to satisfy the requirements imposed by the methods used in the detection tool.

The pre-processing algorithm implemented is based on previous work that makes PMU data a pre-process of archived data off-line [13]. Since the tool is developed for online applications, modifications are introduced in the algorithm

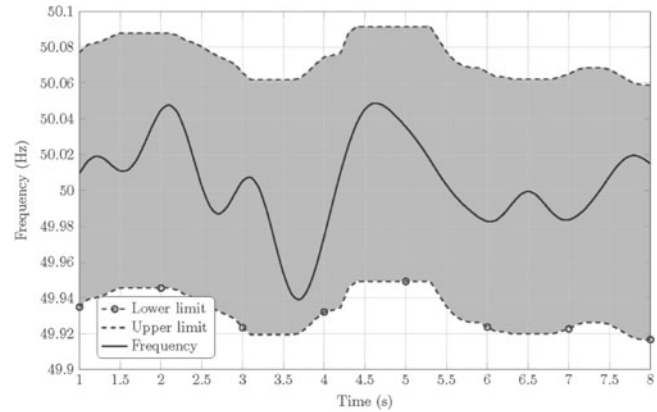


**FIGURE 4.** Example of a confidence interval for the frequency.

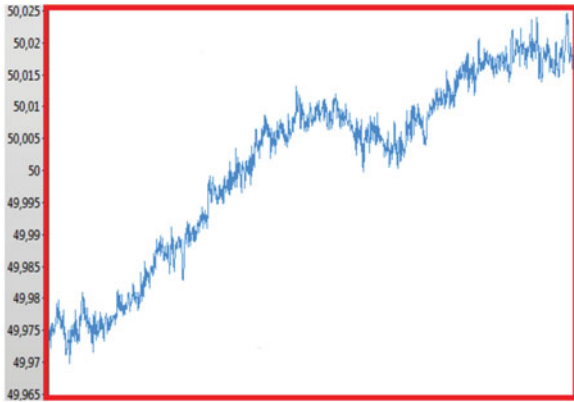
implemented in Monitoring Tool for allowing process of real-time measurements.

In general, the variation of frequency in a power system is the result of the interaction between varying loads and the generation that follows the same variations with an inertial delay. It should thus be a rather smooth process that implies that any value is expected to be within a confidence interval, as shown in Fig. 4, which can be determined from neighboring values and intrinsic system properties. The performance of the outlier removal algorithm is determined by the level of confidence of the interval used.

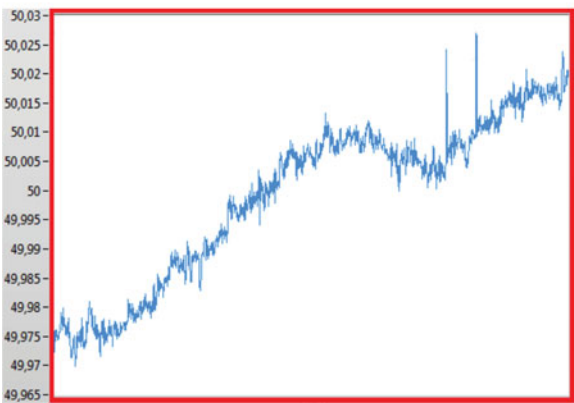
The confidence interval suggested here is built according to the following steps:

1. The input signal: ( $f$ ).
2. Create one copy ( $A$ ) of the input signal delayed by ten samples:  $A_i = f_{i+10}$ , where  $i$  is the time index.
3. Filter one copy ( $M$ ) of the input signal with a moving average filter of order equal to 20:  $M_i = \frac{\sum_{0 < t < 20} f_{i-t}}{20}$ .
4. Subtract ( $M$ ) from ( $A$ ). The combination of a delayed copy ( $A$ ) and ( $M$ ) is equivalent to a having a moving average filter, where the average is computed on the ten preceding samples and nine following samples. Compute the standard deviation  $\sigma$  of the resulting signal.
5. Create the upper ( $U$ ) and lower ( $L$ ) limits of the confidence interval by adding/subtracting  $k\sigma$  to ( $M$ );  $k$  the sensitivity factor, is set by the user.

Each element of ( $A$ ) is then compared to ( $U$ ) and ( $L$ ). If  $U_i > A_i > L_i$ ; the element is preserved; else, it is dropped and will be replaced by an interpolated value. The interpolation is performed by taking as inputs the elements of the signal, the indexes of these elements, and all the indexes at which an element will be returned. Each returned element is either an



(a)



(b)

**FIGURE 5.** Screenshots of the frequency signal with and without outlier removal, drawn in Hertz: (a) outlier removal inactive and (b) outlier removal active.

input element if its index is on both lists or an interpolated value if its index is only on the second list. The chosen method for interpolation is linear; negligible divergences were obtained when comparing with higher-order polynomials.

An example of the outlier removal algorithm in action on real-time PMU data is shown in Fig. 5. The data points removed are single points far from the neighboring values, likely corresponding to measurement errors. The outlier removal effectively performs the above-described tasks.

After removing outliers, the signal is processed further to feed the frequency estimation algorithms by mean removal and high-pass filtering. This aids to attenuate frequency components related to the action of generator governors and loads, which are close to 0 Hz and lower than electro-mechanical modes.

Furthermore, according to Shannon's theorem, all the frequency content below frequency  $f_1$  can be restored if the sampling frequency is at least  $2 \times f_1$ . The typical reporting frequencies of PMUs are 30, 50, or 60 Hz, which correspond to

highest observable frequencies 15, 25, or 30 Hz. The observed frequency in the tool can be much lower; thus, a step of down-sampling is added to remove redundant data (down-sampling is applied for frequency estimation and not performed in the oscillation detection algorithm to avoid lowering the reaction times of the algorithm). This step is preceded by a low-pass filter acting as an anti-aliasing filter.

The implementation was carried out with a band-pass filter for each frequency range configured. The down-sampling factor is calculated from the cut-off frequency of the band-pass filter, considering Shannon's criterion. An upper limit equal to ten was added to the down-sampling factor, motivated by the limited size of the rolling window of buffered data.

### 3. MONITORING APPLICATION

The Monitoring Tool has been implemented as a real-time graphical analysis tool, which could be used by system operators or wind farm owners. LabView was chosen as the software development environment because of the availability of real-time mediators, namely Statnett's Synchrophasor Development Kit [14] and BableFish [15]. In addition, LabView also allows designing a graphical user interface (GUI) in a straightforward manner.

The tool is provided with real-time PMU measurements, allowing monitoring of oscillatory events at a frequency up to the Nyquist limit. This broad frequency spectrum contains different categories of phenomena, mentioned in Section 2. The tool has been implemented for monitoring four frequency ranges simultaneously. The elements in four instances are called *Modules*. The resulting GUI is depicted in Fig. 6.

The graph on the top right of the interface is a simple representation of the buffered input signals received. The signals are displayed one at a time, letting the user choose from the list box on top of the graph in Fig. 6 (the voltage magnitude is displayed in this case). This graph is also useful for calibrating the outlier removal algorithm.

The top left part of the GUI is used to configure the tool and divided into five tabs. The first tab, *Options*, gathers the general configuration of the tool as well as state indicators. The remaining tabs, *Module 1* to *4*, are four identical tabs used for the configuration of the estimation and detection modules; see Fig. 7. The configuration should be done after launching and initializing the tool.

Figure 7 presents an interface with two separate blocks. The block on the left is used to configure the band-pass filter, the parameters are common for both the *Oscillation Detection* and the Frequency Estimation algorithms. The block on the right is dedicated to the Frequency Estimation algorithm and contains the parameters for each of the methods mentioned in Section 2. It also includes the parameters for spectral averaging. Finally,

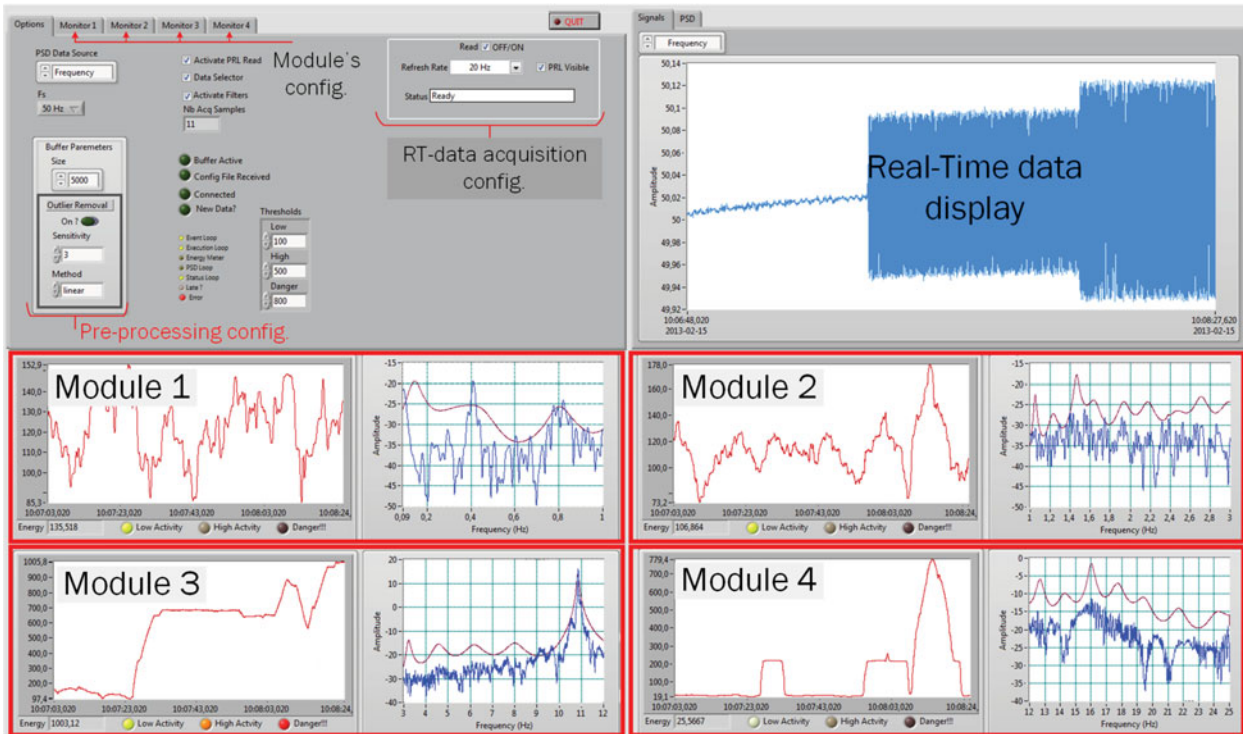


FIGURE 6. Screenshot of the GUI of the Monitoring Tool.

the user is able to choose in the list box if both methods are to be used simultaneously or just one of them.

Once the configuration is set, the outputs of the algorithms are displayed in a Module, highlighted in Fig. 6. The graph on the right presents the PSD, which is the output of the Frequency Estimation algorithm. It is scaled according to the parameters of the band-pass filter, highlighting the content of interest.

The graphical display on the left has several components, the most important are the three indicators *Low Activity*, *High Activity*, and *Danger!!!*, corresponding to the three thresholds defined in the general configuration tab. The comparison is made on the latest sample, whose value is displayed by the field

*Energy*. The graph provides a history to easily corroborate the energy computed with the input signal displayed. Given that the input signal is filtered by three finite impulse response (FIR) filters, the output signal is shorter than the input signal. Moreover, the order of the filters have a strong influence on the length of the output signal. This can be modified by the user to adapt to their needs, measurement features, and particular power network.

In the next section, the Monitoring Tool presented in this article is compared against an in-house tool developed by OG&E. OG&E's tool deployed on a production-grade server is shown in Fig. 8; it provides detection of the oscillations and e-mail notifications. The application was developed in VB.net and utilizes the digital signal processing exocortex (<http://www.exocortex.org/dsp>) library for FFT oscillation detection. It is configured via a set of parameters, that can be tested against archived data for assessing their relevance.

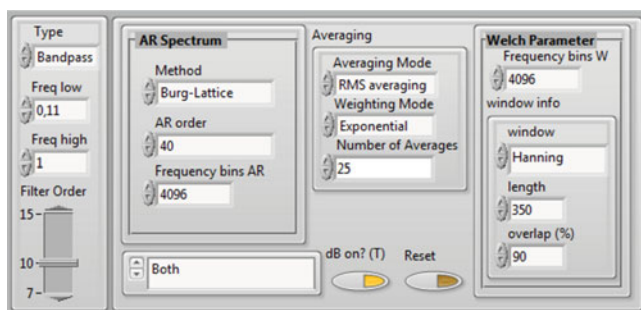


FIGURE 7. Screenshot of the configuration tab of one module of the Monitoring Tool.

## 4. VALIDATION EXPERIMENTS

### 4.1. Replay Experiments

In the previous section, the Monitoring Tool was introduced and all the options for its configuration presented. While the options related to communication connectivity aspects do not require knowledge about the power system analyzed, the

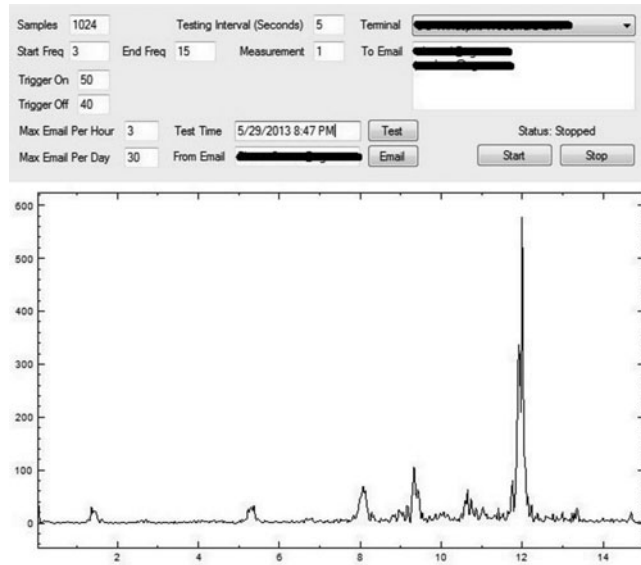


FIGURE 8. Screenshot of OG&E's FFT tool.

configuration of the processing algorithms, especially for frequency estimation, have to be configured according to the properties of the power system. A good solution is to use archived data to calibrate the algorithms.

The original idea was to replay archived data from a phasor data concentrator (PDC), broadcast it as an output stream, and use the Monitoring Tool. The diversity of archival techniques and file structures raised the issue that a PDC, such as OpenPDC [16], was not suitable to replay the archived data format available. This led to the development of the *Replay Tool*.

#### 4.1.1. Replay Tool

The Replay Tool was developed using the same code as the real-time tool. However, additional software was developed to buffer the input measurements from archived data and mimic real-time streams. The interface is almost identical to the Monitoring Tool, as shown in Fig. 9. The processing algorithms are identical. This tool has specific additional features. For example, it allows scrolling along the replayed data, which can be useful to get a quick overview of the content of the selected file. The Replay Tool works, otherwise, exactly like the Monitoring Tool.

#### 4.1.2. Results

The experiments carried out with the Replay Tool used archived data obtained from OG&E, containing measurements from different locations during oscillatory events at a frequency around 13 Hz, as mentioned in the Section 1. These experiments served, during the development and implementation of the algorithms, to verify that the algorithms

worked properly and to calibrate their configurations for other experiments.

Figure 9 presents the Replay Tool during the replay of such oscillatory event. The beginning of the oscillatory phenomenon can be clearly identified in the frequency (display on the top left), as well as in both active and reactive power (displays on the top right). It can also be noticed that the Module on the bottom right, corresponding to the frequency range 12–15 Hz, that the Danger!!! indicator is activated only a few seconds after the beginning of the phenomenon. Additionally the oscillatory frequency is identified to 2 Hz on the PSD.

Figure 8 presents OG&E's tool analyzing the same archived data. As it can be seen on the screenshot that a strong oscillatory activity, above the defined threshold, is occurring at 12 Hz. Additional oscillatory components can be noticed around 1.4, 5.5, 8, 9.4, and 10.7 Hz. The main 12-Hz component is also detected using the Monitoring Tool and it activates the Danger!!! indicator as shown in Fig. 9. All the other components can also be identified in Fig. 9, validating the Monitoring Tool's algorithms.

It must be noted that the OG&E's tool polls a database within fixed time intervals and performs FFT computations using a large buffer; meanwhile, the PMU-based application tool developed uses real-time measurements (small data buffer) and is thereby able to detect the oscillation earlier. This demonstrates the technical advantage of using real-time PMU measurements for fast detection of sub-synchronous oscillation dynamics.

## 4.2. HIL Testing at Smart Transmission System Laboratory (SmarTS) Lab

The experiment presented in this section was carried out at SmarTS-Lab for testing the tool's performance using real-time PMU measurements under different power system conditions. The testing approach utilizes an HIL simulation, which involves the development of a power system model capable of generating the oscillatory phenomenon mentioned in Section 1 and depicted in Fig. 1, as well as additional grid operation scenarios. The Laboratory set-up, as well as some results from the testing experiments, are presented in this section. A desired description of the testing experiments was presented in [17, 18].

### 4.2.1. Setup at SmarTS-Lab

The test setup built in the laboratory makes use of an HIL simulation, replacing the power system by models executed in real-time on a simulator equipped with reconfigurable analog inputs/outputs. The rest of the wide-area monitoring



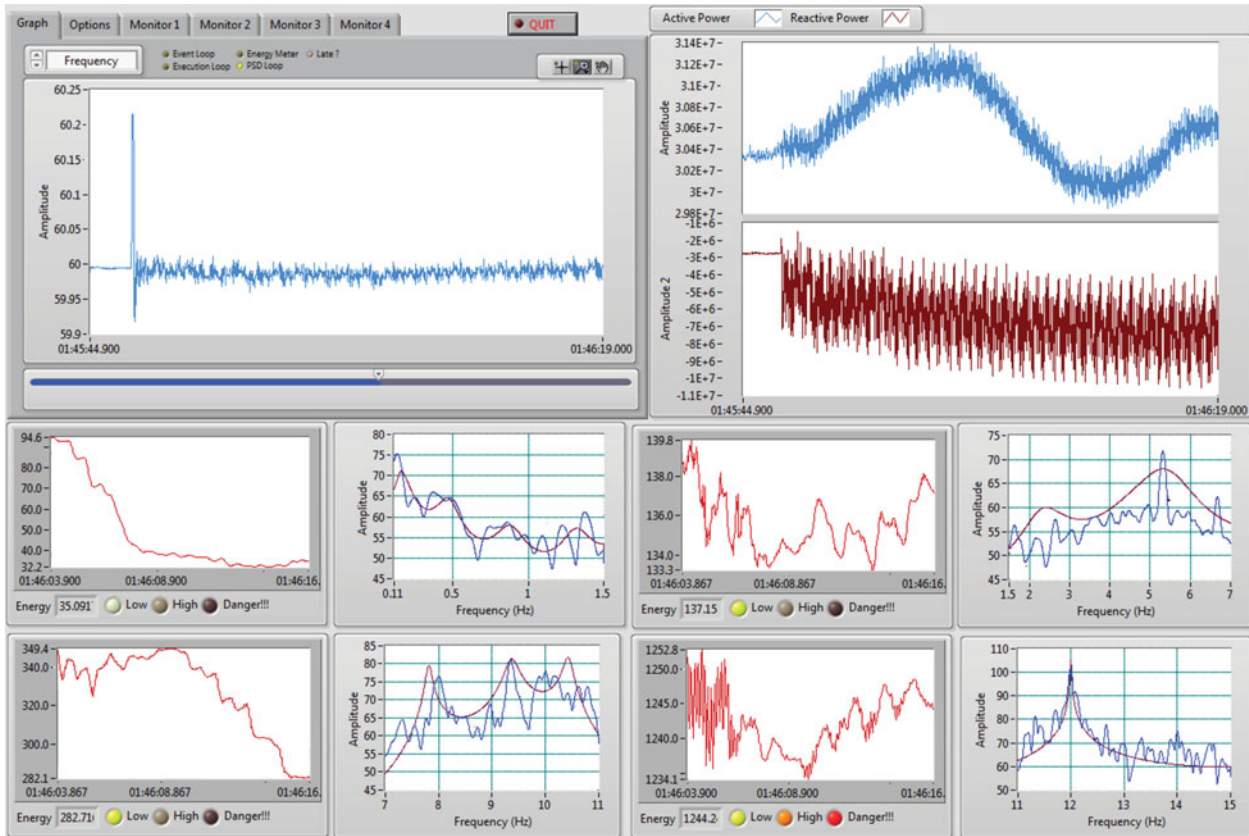


FIGURE 9. Screenshot of the Replay Tool reading the file of the oscillation case at OG&E shown in Fig. 8.

system (WAMS) architecture is replicated, building a testing platform, which is depicted in Fig. 10, with the following elements:

- the real-time simulation target from Opal-RT [19];
- a National Instruments compact reconfigurable Input-Output (cRIO) PMU connected to the analog outputs of the simulator;
- the connection cables of the PMU for acquiring voltage measurements, connected to the simulator;
- the network connection of the PMU to stream the data to the PDC server of the lab;
- the PDC server of the lab, running software from Schweitzer Engineering Laboratories, Inc. (SEL); and
- the application host workstation with the software development environment used to develop the Monitoring Tool [14].

For a complete description of the HIL environment at SmarTS Lab, refer to [20].

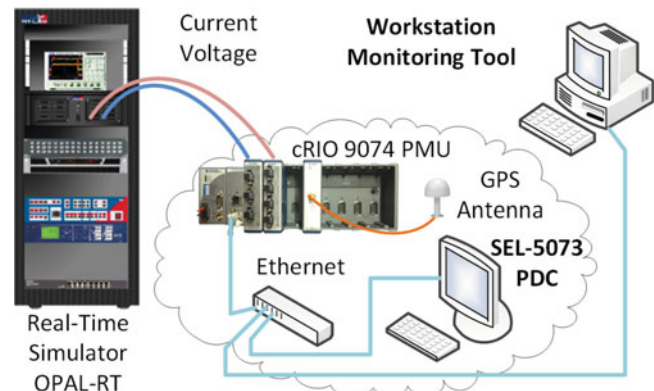
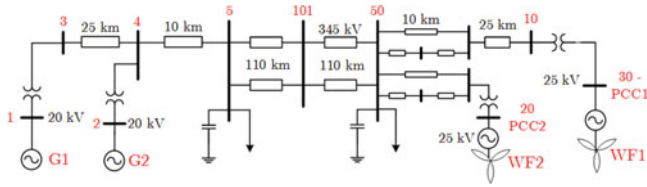


FIGURE 10. Diagram of the experimental set-up at SmarTS-Lab for WAMS application development and testing.

The real-time simulator enables the simulation of different grid operation scenarios and allows the measuring equipment to be interfaced to any of the buses simulated. The PMU measurements gathered in the PDC server are made available in the software development environment through a real-time data mediator, namely Statnett's synchrophasor



**FIGURE 11.** One-line diagram of the test power system with two windfarms.

software development kit (SDK) [14] or BableFish [15]. The data mediators are compliant with the IEEE C37.118.2 Standard [21] for PMU data exchange and deliver the PMU measurements in the chosen software development environment (LabView).

#### 4.2.2. Real-time Simulation Model

For analyzing sub-synchronous oscillations, an adapted version of the well-known Kundur's model benchmark is used. This model is modified by substituting 2 synchronous generators by wind farms containing 13 and 16 DFIG-wind turbines, as shown in Figs. 11 and 12. The important modification was the addition of a variable three phase source, which was used to introduce any type of waveforms into the network as perturbation, thus reproducing similar oscillations as these observed at OG&E. The three-phase source was connected at the point of common connection of the first windfarm to the grid (PCC1 on Fig. 11).

#### 4.2.3. Results

Figure 6 depicts the behavior of the tool when the oscillations are injected with an initial amplitude of 0.05 p.u. followed by an increase of the oscillations amplitude to 0.07 p.u. The resulting system dynamics can be seen on the real-time display,

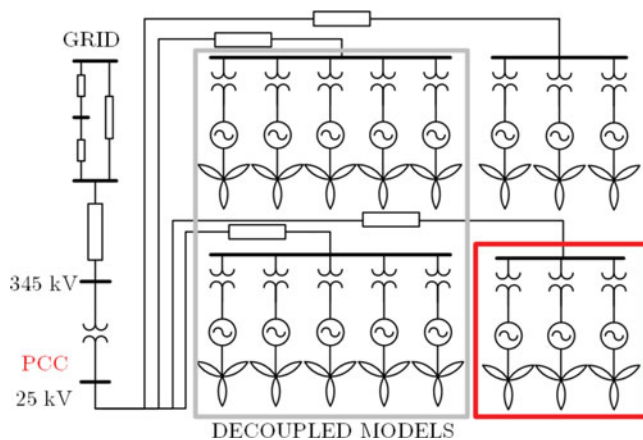


**FIGURE 12.** One-line diagram of the windfarms. The part circled in red is not present in the second windfarm.

where the beginning of the oscillations and the increase of their amplitude can be clearly identified (The oscillations are injected at 10.83 Hz, the equivalent of 13 Hz in a 50 Hz system; This aims to model the original case that happened in the United where the system frequency is 60 Hz.). The results of the processing algorithms are presented in Module 3. It can be noticed on the left part of the Module that the detection of the oscillation has been rapidly achieved. Following the increase of the oscillations' amplitude, the level of energy computed has raised accordingly and all the LED indicators are activated. On the right part, the PSD shows an active frequency identified as 10.83 Hz, confirming the efficiency of the tool for this oscillation case.

### 4.3. Validation Using Hardware-Based Emulation

The last experiment for validating the Monitoring Tool's performances was carried out at the Catalonia Institute for Energy Research (IREC) in Barcelona, Spain. The lab is equipped with a small replica of a utility-connected microgrid [22], comprised of several grid emulators that can generate any variable AC power ( $P_{max} = 4000W$ ). A brief overview of the experiments will be covered in this section, the experimental setup will be presented, and the result of one experiment will be shown. A full description of the validation methods and experiments was presented in [23].

#### 4.3.1. Experimental Setup at IREC: Microgrid

The validation experiments aimed to validate the performance of the developed software under a more realistic testing environment. Thus, the real-time simulator, in the set-up at SmarTS-Lab presented in Section 4.2, was replaced by one of the power emulators mentioned previously. The measurement equipment, as well as the communication architecture, was replicated at IREC, building a full setup, as presented in Fig. 13.

The emulator was configured to inject power oscillations into the distribution grid. The cRIO PMU was connected for both voltage and current measurements to the output of the emulator.

#### 4.3.2. Results

The microgrid at IREC is connected to the Spanish national grid, which is a strong grid when considering the ratings of the microgrid laboratory. Thus, the frequency and voltage are externally controlled, and the Monitoring Tool was adapted to feed the oscillation detection algorithms with current measurements. Also, the real-time data display provides the active and reactive power as they give the most information about the injected oscillations. The screenshots presented in this section

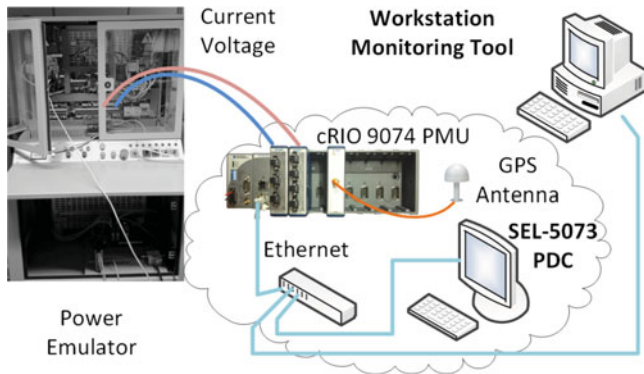


FIGURE 13. Diagram of the experimental setup at IREC.

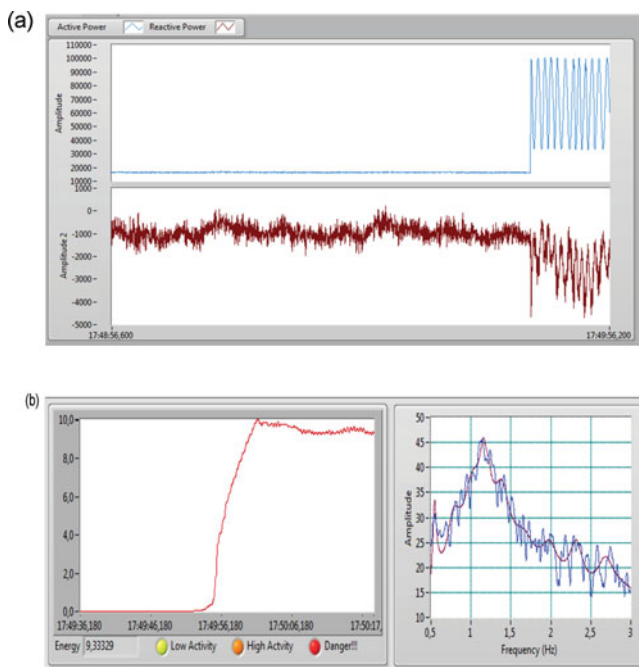


FIGURE 14. Partial screenshot of the Monitoring Tool at the beginning of the injection of oscillations at 1 Hz: (a) active/Reactive power and (b) *Module*-(0.5–3 Hz).

will, therefore, differ from the results presented in Section 4.2 (slightly).

The experiment presented in this article is the first validation experiment, which was designed with respect to the capability of the emulator. The microgrid was conceived to emulate certain equipment that exhibits slow dynamics. The power injection was therefore done with a sinusoidal profile at a frequency of 1 Hz.

Figure 14 presents the results of this experiment. It can be noticed that once the thresholds have been calibrated, the detection is achieved in a few seconds. The frequency of the oscillations is detected around 1.1 Hz (see Fig. 14(b)); this

difference between the reference frequency and the identified frequency is due to errors in the accurate reproduction of the reference signal by the emulator.

## 5. CONCLUSION

This article has presented the design and experimental validation of a PMU-based application for detecting sub-synchronous oscillations at wind farm levels. The application tool introduced provides both the frequency and severity of the oscillation detected. To enhance the tool accuracy and its potential used, sub-synchronous oscillation modes have been classified by the frequency range. Also, the application includes an energy measure of the oscillation detected. The tool has been developed for fast detection of sub-synchronous oscillation dynamics, taking advantage of real-time data obtained from PMU devices.

The PMU-based fast real-time oscillation detection tool has been validated by means of three different cases. First, it has been compared with the existing OG&E tool by the off-line reproduction of the same signal profiles, both obtained the same frequency results, but the PMU-based tool presented also showed the impact of each frequency observed. Finally, the application has been verified in two on-line real-time testings, demonstrating its good performance and accuracy over real measurements.

Additionally, the development of this PMU application showed that new applications can be conceived and implemented without relying on a monolithic software environment and within a relatively short time. The presented PMU-based application not only provides similar results to existing tools but also is capable to detect the sub-synchronous oscillations sooner than the traditional FFT-based tools (with a large data buffer) due to the real-time measures, which require a small data buffer speeding up the data analysis.

## FUNDING

The research was supported partly by European Institute of Innovation and Technology, Knowledge & Innovation Community (EIC KIC) InnoEnergy “Smart Power Project” under Action 2.6 “PMU-based power system tools,” Nordic Energy Research through the STRONG<sup>2</sup>rid project, Statnett SF, the STandUP for Energy Collaboration Initiative.

## REFERENCES

- [1] James F. Manwell, J. G., McGowan, J. G. and Rogers, A. L., *Wind Energy Explained: Theory, Design and Application*, John Wiley & Sons, 2010.

- [2] Milborrow, D., "Europe 2020 wind energy targets, EU wind power now and the 2020 vision," *Windpower Monthly Special Report*, Kingston upon Thames, UK, March 2011.
- [3] U.S. Energy Information Administration (EIA), "Most states have renewable portfolio standards," Feb 2012, available at: <http://www.eia.gov/todayinenergy/detail.cfm?id=4850>.
- [4] Wiik, J., Gjerde, J. O., and Gjengedal, T., "Impacts from large scale integration of wind energy farms into weak power systems," *Proceedings of the International Conference on Power System Technology*, Vol. 1, pp. 49–54, Perth, WA, Australia, 2000.
- [5] White, A., and Chisholm, S., "Relays become problem solvers," *Transm. Distribut. World*, November 2011.
- [6] White, A., Chisholm, S., Khalilinia, H., Tashman, Z., and Venkatasubramanian, M., "Analysis of subsynchronous oscillations at OG&E," *NASPI-NREL Synchrophasor Technology and Renewables Integration Workshop*, Denver, CO, 7 June 2012.
- [7] Hauer, J. F., and Vakili, F., "An oscillation detector used in the BPA power system disturbance monitor," *IEEE Trans. Power Syst.*, Vol. 5, No. 1, pp. 74–79, Feb. 1990.
- [8] Trudnowski, D., "Fast real-time oscillation detection," Proceedings North American SynchroPhasor Initiative (NASPI) Work Group Meeting, Orlando, FL, February 29–1 March 2012.
- [9] Welch, P., "The use of fast Fourier transform for the estimation of power spectra: A method based on time averaging over short, modified periodograms," *IEEE Trans. Audio Electroacoustics*, Vol. 15, No. 2, 70–73, June 1967.
- [10] Vanfretti, L., Bengtsson, S., Aarstrand, V., and Gjerde, J. O., "Applications of spectral analysis techniques for estimating the Nordic grid's low frequency electromechanical oscillations," *16th IFAC Symposium on System Identification*, pp. 1001–1006 Brussels, Belgium, July 2012.
- [11] Sanchez-Gasca, J., "Identification of electromechanical modes in power systems," (Technical Report PES-TR15, formerly TP462), *IEEE Power & Energy Society*, June 2012.
- [12] Hayes, M. H., *Statistical Digital Signal Processing and Modeling*, John Wiley & Son, 1996.
- [13] Vanfretti, L., Bengtsson, S., and Gjerde, J. O., "Preprocessing synchronized phasor measurement data for spectral analysis of electromechanical oscillations in the nordic grid," *Int. Trans. Electr. Energ. Syst.*, Vol. 25, pp. 348–358. doi: 10.1002/etep.1847.
- [14] Vanfretti, L., Aarstrand, V. H., Almas, M. S., Peric, V. and Gjerde, J. O., "A software development toolkit for real-time synchrophasor applications," *Proceedings of IEEE PowerTech 2013*, pp. 1.6, Grenoble, France, 16–20 June 2013. doi: 10.1109/PTC.2013.6652191
- [15] Vanfretti, L.; Al Khatib, I.; Almas, M.S., "Real-time data mediation for synchrophasor application development compliant with IEEE C37.118.2," *2015 IEEE Power & Energy Society Innovative Smart Grid Technologies Conference (ISGT)*, pp.1–5, Washington, USA, 18–20 February 2015. doi: 10.1109/ISGT.2015.7131910
- [16] "OpenPDC: The open source phasor data concentrator," available at: <http://openpdc.codeplex.com/>
- [17] Vanfretti, L., Baudette, M., Al Khatib, I., Almas, M. S. and Gjerde, J., "Testing and validation of a fast real-time oscillation detection PMU-based application for wind-farm monitoring," *First International Black Sea Conference on Communications and Networking*, Batumi, Georgia, July 2013.
- [18] Baudette, M., *Fast Real-Time Detection of Sub-synchronous Oscillations in Power Systems Using Synchrophasors*, Master's Thesis, KTH, Electric Power Systems, Stockholm, Sweden, 2013.
- [19] "eMEGAsim PowerGrid Real-Time Digital Hardware in the Loop Simulator—Opal RT," available at: <http://www.opal-rt.com/>
- [20] Almas, M.S., Baudette, M., Vanfretti, L., Lovlund, S., and Gjerde, J.O., "Synchrophasor network, laboratory and software applications developed in the strong2rid project" *2014 IEEE PES General Meeting/Conference Exposition*, pp. 1–5, Washington, USA, July 2014.
- [21] IEEE, "IEEE standard for synchrophasor data transfer for power systems," *IEEE Standard C37.118.2-2011 (Revision of IEEE Std C37.118-2005)*, pp. 1–53, 2011.
- [22] Ruiz-Alvarez, A., Colet-Subirachs, A., Alvarez-Cuevas, F., Gomis-Bellmunt, O., and Sudria-Andreu, A., "Operation of a utility connected microgrid using an IEC 61850-based multi-level management system," *IEEE Trans. Smart Grid*, Vol. 3, No. 2, pp. 858–865, 2012.
- [23] Baudette, M., Vanfretti, L., Del-Rosario, G., Ruiz-Alvarez, A., Dominguez-García, J. L., Al-Khatib, I., Shoaib Almas, M., Cairo, I., and Gjerde, J. O., "Validating a real-time PMU-based application for monitoring of sub-synchronous wind farm oscillations," *IEEE PES. Innovative Smart Grid Technologies Conference North America (ISGT North America)*, Washington, USA, February 2014.

## BIOGRAPHIES

**Luigi Vanfretti** received his E.E. degree from Universidad de San Carlos de Guatemala, Guatemala, in 2005 and his M.Sc. and Ph.D. in electric power engineering from Rensselaer Polytechnic Institute, Troy, NY, USA, in 2007 and 2009, respectively. He was a visiting researcher with University of Glasgow, Glasgow, Scotland, in 2005. He became an assistant professor at KTH Royal Institute of Technology, Stockholm, Sweden, in 2010; he was conferred the Swedish title of "Docent" in 2012 and obtained a tenured associate professor position in 2013, which he currently holds. He also serves as a special advisor in R&D strategy and international collaboration for the Research and Development Division of Statnett SF, the Norwegian transmission system operator, where he has worked since 2012. His research interests are in the general area of power system dynamics, while his main focus is on synchrophasor applications.

**Maxime Baudette** is a Ph.D. student in the Electric Power Systems Department at the KTH Royal Institute of Technology, Stockholm, Sweden. He received the M.Sc. in electrical engineering from KTH (Sweden) and Supélec (France) in 2013. He is a member of the SmarTS-Lab research group at KTH. He has keen interest in real-time simulations; the HIL approach; and wide-area monitoring, protection, and control (WAMPAC).

**José-Luis Domínguez-García** received his B.S. and M.S. in industrial engineering from the School of Industrial Engineering of Barcelona, Technical University of Catalonia, Barcelona, Spain, in 2009. He developed his master's thesis in Oulun Yliopisto, Oulu, Finland. In 2013, he received his Ph.D. in electrical engineering from UPC with a qualification of excellent "Cum Laude." He received the Outstanding Ph.D. Thesis Award from UPC in 2015. Since 2010, he has been a researcher in the Catalonia IREC. He was an academic visitor of the Institute of Energy, Cardiff University, Wales, UK, in 2011. His research interests are modeling and control of electrical machines and power converters, renewable energy integration in power systems, power system dynamics, and linear system theory.

**Muhammad Shoaib Almas** is a Ph.D. candidate at the Electric Power Systems Division of KTH Royal Institute of Technology, Stockholm, Sweden. He received his M.Sc. and B.E. in electrical power engineering from KTH (Sweden, 2011), and National University of Sciences and Technology (NUST) (Pakistan, 2007) respectively. He is a member of the SmarTS-Lab research group at KTH. He has been interested in real-time simulations, the HIL approach, substation automation, WAMPAC, internetworking, and cybersecurity.

**Austin White** is a lead engineer at OG&E in Oklahoma City, OK, USA. He is currently responsible for transmission/substation protective system settings and coordination, disturbance event/misoperation analysis, and system modeling/simulation. Recently, he has been leading the efforts to deploy a synchronized phasor measurement system for OG&E. He received his B.S. in electrical engineering from Oklahoma Christian University in 2001, followed by his M.S. in engineering and technology management from Oklahoma State University in 2008. He is also a licensed Professional Engineer in the state of Oklahoma.

**Jan Ove Gjerde** was born in Hareid in 1958. He received his M.Sc. in electrical engineering from the Norwegian Institute of Technology in 1983. He has long experience in R&D from the energy sector, both as a senior research scientist at Sintef Energy Research and as a department head at ABB Corporate Research, Power System and Components Department. From 2011–2013, he served as vice president of R&D at Statnett and was responsible for developing R&D strategies for the overall R&D programs at Statnett, in particular, for use on new concepts for risk management, wide area monitoring system (WAMS), wide area control system (WACS), and wide area protection systems (WAPS), and the overall R&D programs at Statnett. He is currently a special advisor in the R&D division of Statnett SF.